Egyptian Journal of Geology

https://egjg.journals.ekb.eg

Relation Between Pore Pressure Evaluation and Hydrocarbon Saturation for Abu Roach Formation in Badr EL-Din 15 Field, Western Desert, Egypt.

A.M. Talaat [1], E. El Sayed [2], M. Ghorab [1], M.A. Ramadan [1], A.Z. Nooh [1]

[1] *Exploration Department, Egyptian Petroleum Research institute, Cairo, Egypt*

[2] *Geology Department, Faculty of Science, Minia university, Minia, Egypt*

BED-15 oil Field which is located in the North-Western region of the Abu Gharadig sedimentary basin within the Egyptian Western Desert. Bed-15 Field spans across latitudes 29° 45' to 30 ° 05' N and longitudes 27° 30' to 28° 10' E and considered a component of the Badr El-Din Concession, which is situated approximately 300 km west of Cairo and around 100 km west of Bed-1 location. Abu Roach Formation is the subject of the research using a combination of petrophysical data, well log analysis, and subsurface geologic studies to understand the potential hydrocarbons in Abu Roach Formation, Badr 15 Field, using 5 wells (Bed15-1, Bed15-3, Bed 15-7, Bed15-8 and Bed15-9) different types of petrophysical parameters (porosity, shale volume and water and hydrocarbon saturations) were determined. Four wells (Bed15-1, Bed15-3, Bed 15-7 and Bed15-9) were selected for evaluating pore pressure of Abu Roach Formation utilizing drilling exponent (Dxc) and wireline logs. A correlation was observed between the pore pressure and the hydrocarbon saturation in the area under investigation.

Keywords: Pore pressure evaluation, Eaton's Resistivity, Drilling exponent, Hydrocarbon saturation, Abu Roach Formation.

1. Introduction

The case study presented in the paper focuses on the Bed-15 oil Field, located in the North-Western region of Abu Gharadig sedimentary basin within Egyptian Western Desert. Bed-15 Field spans across latitudes 29° 45' to 30 ° 05' N and longitudes 27° 30' to 28° 10' E. (**Fig.1**) and considered a component of Badr El-Din Concession, which is situated approximately 300 km west of Cairo and around 100 km west of the Bed-1 location.

The process of designing and analyzing a well involves evaluating the pressures within the Formation. It is crucial to determine the pore pressure in order to optimize the density of the drilling mud and ensure sufficient overbalance, while also maintaining the integrity of the formation. Understanding the pore pressure is vital for achieving the right mud density that provides adequate overbalance without surpassing the fracture pressure of the formation. By considering these factors, we can drill a well safely and cost-effectively. The main objective of the present research is to integrate subsurface geological investigations, formation pressure assessment, and well log analysis in order to enhance our comprehension and exploit the hydrocarbon prospects in Badr El-Din 15 oil Field. 5 wells were selected (Bed15-1, Bed15-3, Bed 15-7, Bed15-8 and Bed15-9) to evaluate Abu Roach Formation in Badr EL-Din 15 Field, Western Desert, Egypt.

2. Geologic Setting

The surface geology of the Western Desert North of latitude 28° is considered of complex nature. The sedimentary sequence in this area has been studied and dated by several authors, e.g. **(Said, 2017), (Hanter ,2017), (Shalaby, 2013), (El Gezeery et al., 1972), (Barakat and Darwish, 1987)** … etc.

*Corresponding author e-mail: fidrix@gmail.com

Received: 04/10/2023; Accepted: 06/11/2023

DOI: 10.21608/EGJG.2023.239036.1057

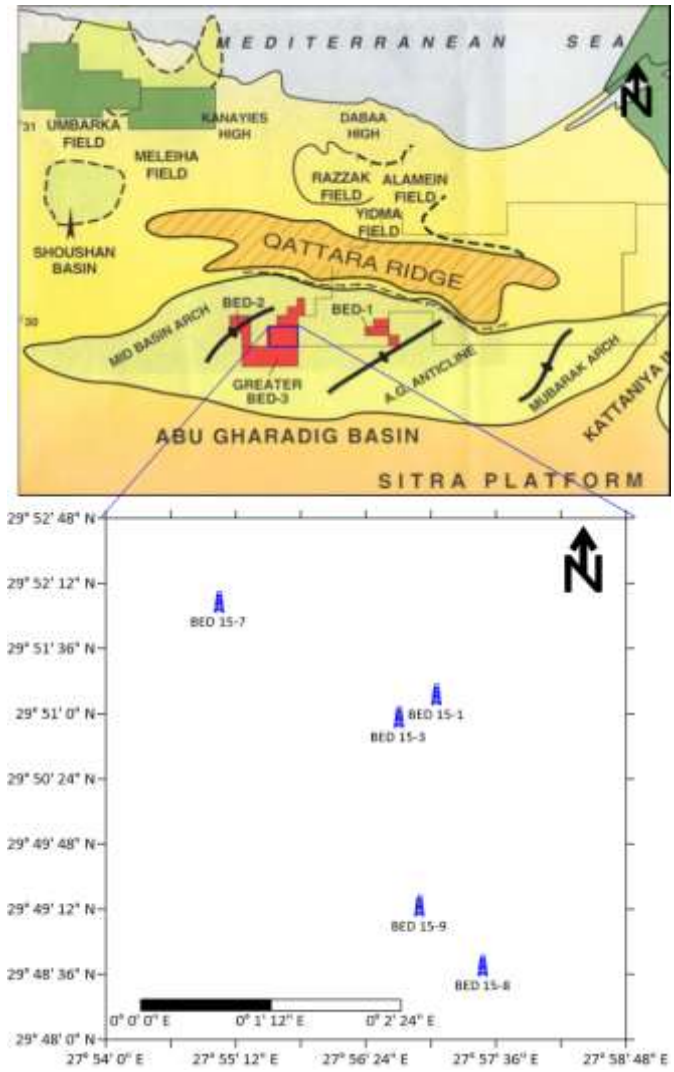

Fig. 1. Location Map of the Study area.

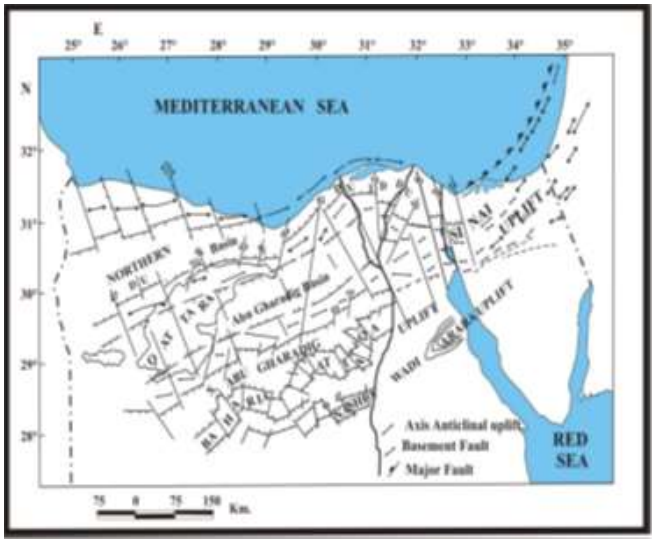

Fig. 2. Basement Tectonic Map of the Northern Western Desert of Egypt (Sultan and Halim, 1988).

The area of study lies in the northern unstable shelf, **(Awad, 1984)** concluded that Qattara Depression Area and its continuation (Abu Gharadig and Fayoum basins) to the Nile Delta were affected by several tectonic events. These geological processes resulted in the Formation of significant faults that extend in an ENE-WSW direction, as well as the accumulation of a substantial amount of Upper Cretaceous sediments. Additionally, another set of faults developed in an east-west direction, which exert control over the northern side of the basin. **(Fig.2).**

(Zante, 1984) and (El Gazzar, 2016) described the primary structural characteristics of Abu Gharadig basin which consist of two half grabens that are divided by a ridge known as the 'Mid basin Arch' oriented in a northeast-southwest direction. The eastern half graben is deeper and larger compared to the western half graben, gradually ascending towards the Sitra platform in the south. It is separated from the northern Qattara ridge by a significant fault zone with an arcuate shape.

According to (Taha, 1992), recent geophysical surveys and well data collected by oil companies conducting exploration activities in the Western Desert have revealed that various sections of the North Western Desert are characterized by Mid-Jurassic to Cretaceous basins that trend in a northeast-southwest and east-northeast-west-southwest direction.

3. Formation Evaluation

Formation evaluation is the core purpose of well log analysis. After completing editing and correcting the data, Shale volume, effective porosity, total porosity, water saturation and hydrocarbon saturation can be estimated **(AZ Noah and T.F. Shazly, 2014).**

3.1 Shale volume estimation

The accurate determination of the shale volume (**Vsh**) is very important for reservoir rock analysis. The assessment of reservoir quality, including petrophysical parameters, lithology identification, porosity, fluid type and distribution, and estimated water cut, primarily relies on the analysis of shale volume. These parameters play a crucial role in accurately evaluating the potential of a reservoir. The Shale volume can be estimated using single shale volume indicators (gamma ray, neutron method and resistivity method) where single curve indicators are depended on the readings of one log for the estimation of the shale volume **(Tarek F. Shazly and Wafaa abd ELaziz, 2010)**.

3.1.1 Gamma ray method:

Shale volume can be estimated from gamma ray log using the following **(Dresser Atlas, 1979), (Schlumberger, 2004)**:

$$\mathbf{V_{cl}\ GR} = \frac{\mathbf{GR\ log - GR\ min}}{\mathbf{GR\ max - GR\ min}} \quad \mathbf{(1)}$$

Larionov older rocks **(Mesozoic):**

$$\mathbf{V_{sh} = 0.333 \times 2^{(2 \times Z)} - 1.0} \quad \mathbf{(2)}$$

Larionov younger rocks **(Tertiary elastics)***:*

$$\mathbf{V_{sh} = 0.08336 \times 2^{(3.7 \times Z)} - 1.0} \quad \mathbf{(3)}$$

$$\textbf{Clavier: } \mathbf{V_{cl}\ GR} = 17 - \sqrt{3.38 - (Z + 0.7)^2} \quad \mathbf{(4)}$$

$$\textbf{Stieber: } \mathbf{V_{cl}\ GR} = \frac{0.5 \times Z}{1.5 \times Z} \quad \mathbf{(5)}$$

3.1.2 Neutron method:

The shale volume can be determined using the neutron method when there is a high clay percentage and a low effective porosity using:

$$\mathbf{V_{sh}} \leq \frac{\Phi N_{log}}{\Phi N_{sh}} = \mathbf{X} \quad \mathbf{(6)}$$

Where, $\mathbf{\Phi N_{log}}$ is the neutron reading for studied zone and $\mathbf{\Phi N_{sh}}$ is the neutron reading of the shale zone.

3.1.3 Resistivity method:

The Shale volume can be calculated using the following equation **(Schlumberger, 1987):**

$$\mathbf{V_{sh}} \leq \left(\frac{R_{sh}}{R_t\ log}\right) - \left(\frac{R_{cl} - R_t\ log}{R_{cl} - R_{sh}}\right)^{1/b} = \mathbf{X} \quad \mathbf{(7)}$$

Where**,** $\mathbf{R_{sh}}$ is the resistivity reading at shale zone, $\mathbf{R_{cl}}$ is the resistivity reading at clay zone, $\mathbf{R_t\ log}$ is the resistivity reading for studied zone and **b** is a constant in which its value varies between 1 and 2.

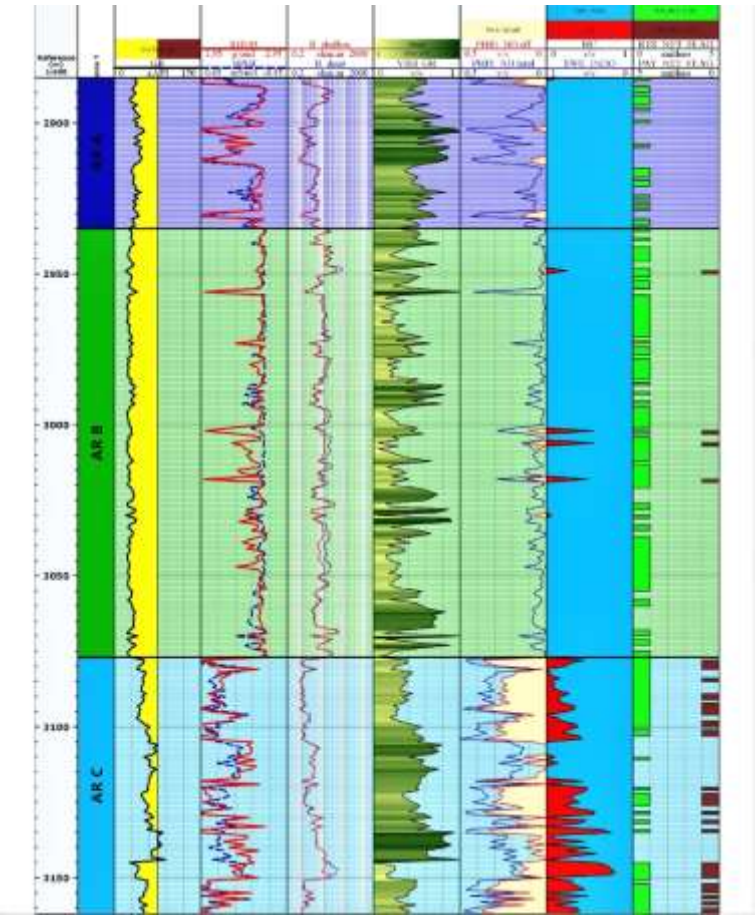

Fig. 3. Lithostratigraphic Crossplot for Bed15-1 well.

By using Techlog program to estimate the shale volume it produced a lithostratigraphic crossplot **(Fig.3).**

3.2 Determination of porosity types:

3.2.1 Total porosity:

Total porosity (**Φt)** refers to the proportion of the entire volume of minerals in a rock to the combined volume of empty spaces, such as pores, fissures and fractures, which are not occupied by solid materials.

One way to determine it is by combining the data from two porosity logs, such as the density and neutron logs. **(Schlumberger, 1972b)**

$$\Phi T = \sqrt{\frac{\Phi NC^2 + \Phi DC^2}{2}} \quad (8)$$

3.2.2 Effective porosity:

The degree to which the rock pores are connected to one another and form channels determines the sort of porosities present. to make the lithologic components' fluid passageways easier **(T.F. Shazly and A.Z Noah, 2012)**.

the effective porosity can be estimated using **(Schlumberger, 1972b):**

$$\Phi_E = \Phi_T (1-V_{sh}) \quad (9)$$

By using Techlog program to estimate total and effective porosity it produced a lithostratigraphic Crossplot **(Fig.3)**.

3.3 Determination of water and hydrocarbon saturations:

Water saturation refers to the portion of pore space in a rock that is filled with water from the Formation. This concept is significant in log interpretation as it aids in determining the amount of hydrocarbon present in a reservoir. The water saturation is estimated in both the uninvaded-zone **(S_w)** and flushed zone **(S_{xo})**. Water saturations in shaly and clean zones are studied by many workers

as (**Archie, 1942), (Simandoux, 1963), Indonesian (Poupon and Leveaux, 1971), (Schlumberger, 1972b), (T.F. Shazly et al, 2013)** and others.

3.3.1 Water Saturation (S_w):

3.3.1.1 Water saturation of uninvaded-zone (S_w):

a- Clean Zone

Archie's formula (1942), is used to determine the water saturation in non-shaly (clean) Formations with consistent porosity, by taking into account the resistivity logs as follow:

$$\mathbf{S_w} = \left[\boldsymbol{F} * \frac{R_w}{R_t}\right]^{\frac{1}{n}} \quad \textbf{(10)}$$

$$\mathbf{F} = \left(\frac{a}{\Phi^m}\right) \quad \textbf{(11)}$$

Where, a is the tortuosity factor, equal to 1 in carbonates, 0.62 in nonconsolidated sands and 0.81 in consolidated sands, according to Humble's work **(Schlumberger, 1987), m** is the cementation factor which is equal to 2 in carbonates and in consolidated sands while it is 2.15 in unconsolidated sands, according to Humble's work **(Schlumberger, l997), n** is the saturation exponent, typically set at 2.0 but ranging from 1.8 to 2.5.

b- Shaly Zones

the following equation might be to determine the water saturation (Sw) within the Shaly Formation. **(Poupon and Leveaux, 1971):**

$$\frac{1}{\sqrt{R_t}} = \left(\frac{V_{sh}{}^{(1-\frac{V_{sh}}{2})}}{\sqrt{R_{sh}}} + \frac{\Phi^{\frac{m}{2}}}{\sqrt{a*R_w}}\right) * \boldsymbol{S_w}^{\frac{n}{2}} \quad \textbf{(12)}$$

3.3.1.2 Flushed zone saturation (S_{xo}):

a- Clean Zones

The water saturation of the flushed zone (**Sxo**) in the clean zones can be used as a gauge of the moveability of hydrocarbons and can be calculated using **Archie's equation**:

$$\mathbf{S_{xo}} = \left[\boldsymbol{F} * \frac{R_{mf}}{R_{xo}}\right]^{\frac{1}{n}} \quad \textbf{(13)}$$

$$\mathbf{F} = \left(\frac{a_2}{\Phi^m}\right) \quad \textbf{(14)}$$

where, $\mathbf{R_{mf}}$ is the resistivity of mud cake and $\mathbf{R_{xo}}$ is the resistivity of mud filtrate.

b- Shaly Zones

The water saturation in the shaly areas can be calculated using the subsequent equation. (**Schlumberger, 2004**):

$$\frac{1}{\sqrt{R_{xo}}} = \left(\sqrt{\frac{\Phi^m}{aR_{mf}}} + \frac{V_{cl}{}^{(1-\frac{V_{cl}}{2})}}{\sqrt{R_{cl}}}\right) \boldsymbol{S_{xo}}^{\frac{n}{2}} \quad \textbf{(15)}$$

Where $\mathbf{S_{xo}}$ is the water saturation in invaded zone.

3.3.2 Hydrocarbon saturation (S_h):

The following formula is utilized to determine the overall hydrocarbon saturation.

$$\mathbf{Sh = 1 - Sw} \quad \textbf{(16)}$$

The water saturation in the uninvaded and flushed zones (**Sw** and **Sxo**) can be used to determine the residual (**Shr**) and moveable (**Shm**) portions of the hydrocarbon saturation as follows:

$$\mathbf{S_{hr} = 1 - S_{xo}} \quad \textbf{(17)}$$

$$\mathbf{S_{hm} = S_h - S_{hr}} \quad \textbf{(18)}$$

The following formula is used to compute the Bulk Volume Hydrocarbon (**BVH**):

$$\mathbf{BVW = \Phi_{eff} * S_{hm}} \quad \textbf{(19)}$$

By using Techlog program to estimate Water and Hydrocarbon saturation, it produced a lithostratigraphic crossplot **(Fig.3)**.

3.4 Distribution of petrophysical parameters of the studied area:

The values of porosity, shale volume, water and hydrocarbon saturations in Abu Roach Formation was distributed both vertically and horizontally across the studied area.

3.4.1 Vertical distribution of petrophysical parameter:

Lithostratigraphic crossplot was plotted for the wells (Bed15-1, Bed15-3, Bed 15-7, Bed15-8 and Bed15-9) using the estimated petrophysical parameters beside gamma ray, neutron, density, deep and shallow resistivity.

These crossplots showed that Abu Roach C member is our reservoir in which it revealed the presence of attainable hydrocarbon in Bed15-1 and Bed 15-3 which it can be produced from, and the presence of unattainable hydrocarbon and water in the other wells (Bed15-7, Bed15-8 and Bed15-9).

3.4.2 Horizontal distribution of petrophysical parameter:

Isoparametric maps were made for the studied area using petrophysical parameters of Abu Roach C member (**Table 1**)

3.4.3 Shale volume distribution map for Abu Roach C:

it shows that the shale volume decreases towards the Centre of the studied area as well as the South-Eastern part **(Fig.4)**

3.4.4 Effective porosity distribution map for Abu Roach C:

it shows that the porosity increases towards the north eastern part of the map **(Fig.5)**

3.4.5 Hydrocarbon saturation map for Abu Roach C:

This map shows that the Hydrocarbon Saturation increases to the central part of the studied area which was in the same direction in which the Shale volume decreases and porosity increases **(Fig.6)**

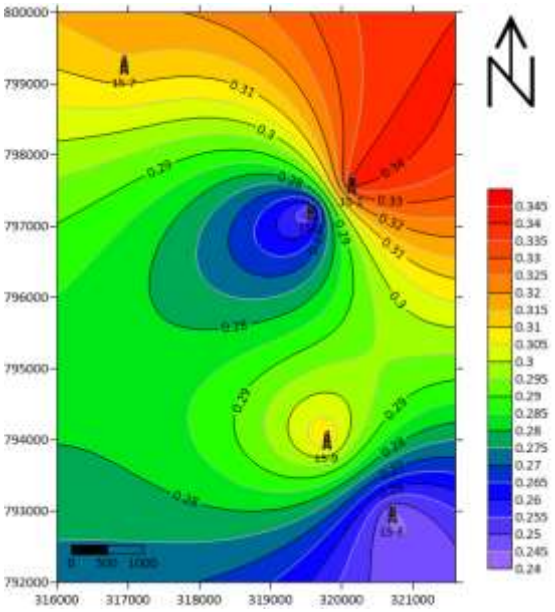

Fig. 4. Shale volume distribution map for Abu Roach C for the studied area.

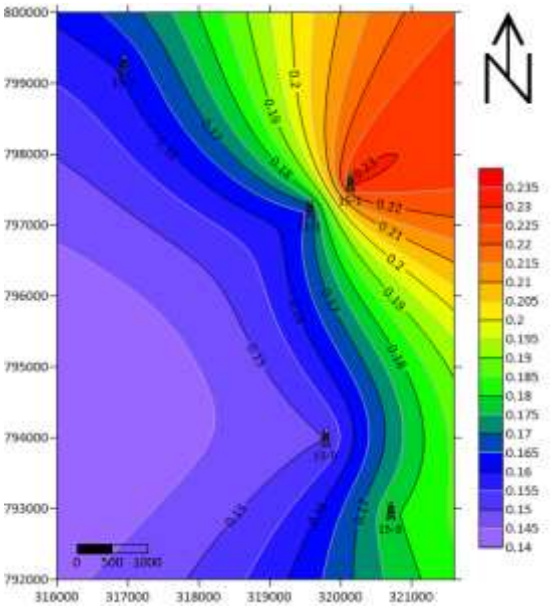

Fig. (5) Porosity distribution map for Abu Roash C for the studied area.

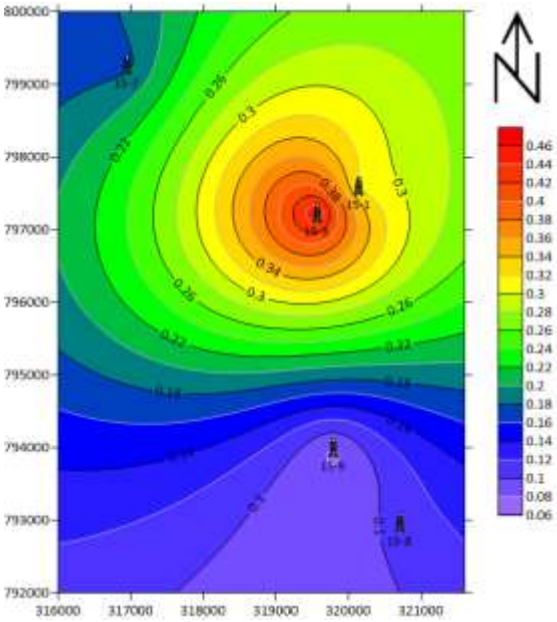

Fig. (6) Hydrocarbon Saturation map for Abu Roach C for the studied area.

Table 1. Reservoir petrophysical parameter of Abu Roach C member.

Well nan	Top	Bottom	Effective porosity	Shale volume	Hydrocarbon Saturation
15-1	3077	3162	0.231	0.342	0.317
15-3	3063	3146	0.166	0.251	0.458
15-7	3165.5	3249.5	0.161	0.314	0.175
15-8	3146	3146	0.179	0.244	0.109
15-9	3125	3209.5	0.15	0.31	0.077

4. Pore pressure evaluation:

Having a grasp of fundamental pressure principles, like hydrostatic pressure, overburden pressure, and Formation pore pressure, is crucial in the Fields of drilling, production, and reservoir engineering. Overburden pressure refers to the force exerted at a specific depth due to the weight of sediment and the fluid it holds. On the other hand, hydrostatic pressure is the pressure exerted by a stationary fluid column at a designated depth. Its magnitude is influenced by the density of the fluid and the vertical height of the column. Lastly, Formation pressure denotes the pressure acting on fluids within the pore spaces of the Formation. The importance of accurately estimating and understanding pore pressure cannot be overstated, as any uncertainties in this measurement can result in a range of issues such as difficulties in removing a stuck pipe, instability problems in the wellbore, damage to Formations, unexpected well kicks, and, in the worst-case scenario, blowouts. Having thorough knowledge of the pore pressure within a Formation is not only crucial for drilling a well that is both safe and cost-effective, but it is also essential for assessing potential risks linked to exploration drilling, including the integrity of seals and the movement of Formation fluids. (**Tang et al., 2011**).

For this study 4 wells (Bed15-1, Bed15-3, Bed15-7 and Bed15-9) were selected from Badr el-Din oil Field to evaluate Pore pressure for Abu Roach Formation.

4.1 Pore pressure estimation:

a) Using Drilling Exponent:

The d-exponent, also known as the drilling exponent, is a method used to standardize and normalize the rate of penetration (**ROP**) in order to determine the drillability or hardness of a Formation. It was introduced for analyzing Formation pore pressure by **(Jorden and Shirley, 1966)** and **(Bourgoyne et.al. 1986).** This method aimed to standardize the parameters of weight on bit (**WOB**), rotary speed (**N**), and bit diameter (**db**) in the Bingham drilling model for calculating ROP. **(Bingham, 1965)** proposed that the general formula for the relationship between bit diameter, rotational speed, weight on bit, and penetration rate is as follows:

$$\left(\frac{\mathbf{R}}{\mathbf{N}}\right) = \mathbf{a}\left(\frac{\mathbf{W^d}}{\mathbf{B}}\right) \qquad \textbf{(20)}$$

Where: **d** is the drilling exponent, **R** is the rate of penetration, **N** is the rotary speed, **W** is the weight on bit, **B** is the bit diameter, **a** is the matrix strength constant.

(Jorden and Shirley, 1966) found a solution for the previous equation by solving for the variable "d". They introduced a constant to enable the use of a common unit in the oilField industry. The results were then plotted on semi-log paper, revealing d-exponent values that were both practical and useful.

$$\mathbf{D}=\frac{\log(\frac{R}{60N})}{\log(\frac{12W}{10^6 B})} \qquad \textbf{(21)}$$

Where: **D** is the drilling exponent, **R** is the rate of penetration, **N** is the rotary speed, **W** is the weight on bit and **B** is the bit diameter (inches)

Then this correction was suggested by **(Rehm and McClendon, 1971 &1973)**

$$\mathbf{Dxc = D\ x}\ \frac{N.FBG}{ECD} \qquad \textbf{(22)}$$

Where: **D** is referring to the drilling exponent, **Dxc** is referring to the corrected drilling exponent, **N.FBG** is referring to the normal Formation balance gradient while **ECD** is referring to the effective circulation density.

b) Using Eaton's Resistivity:

One of the first techniques for wireline detection was resistivity, which gauges a Formation's electrical current-conducting ability. Typically, the solid material does not allow electricity to flow through it, but the empty spaces within can contain either conductive salt water or non-conductive

hydrocarbons. The composition and volume of the fluid in these spaces determine how porous the material is and therefore affect its resistivity measurements. If the clay Formation remains consistent and the properties of the fluid do not change, a decrease in resistivity measurement will correspond to an increase in porosity and thereby result in increased pressure. According to **(Hottman & Johnson, 1965)**, a straightforward equation can be used to depict the relationship between normal and anomalous pressure in clays.

$$R_o/R_n \quad (23)$$

Where: R_o refers to the observed or measured resistivity, R_n refers to the resistivity that is typically observed in rock at the investigated depth under normal pressure.

(Eaton, 1975) produced the following equation by incorporating the exponent of 1.5 into the pore pressure equation:

$$P_o = S - (R_o/R_n)1.5(S-P_n) \quad (24)$$

Where: P_o refers to the Pore Pressure gradient, P_n refers to the Normal Pore Pressure gradient and **S** refers to the Overburden Stress gradient.

Further analysis (**Eaton, 1975)** suggested changing the exponent value to 1.2. thus became:

$$P_o = S - (R_o/R_n)1.2(S-P_n) \quad (25)$$

The normal compaction trend (NCT) is placed onto the log after resistivity logs for clay are plotted against depth to get the normal resistivity. Therefore, R_n refers to the value on the NCT at depth from which to compute pore pressure. Indicated by the contrast between R_o and R_n is how different the actual porosity at that depth is from genuine porosity.

4.2 Pore pressure evaluation:

After estimating pore pressure using drilling exponent and Eaton's resistivity, results were plotted on a lithostratigraphic Crossplot **(Fig.7)** which showed that the area is divided into 3 zones in which Abu Roach A is considered the seal as it consist of impermeable shale and has a normal pressure zone while Abu Roach B is considered as a transition zone as it consists of limestone, shale and sandstone intercalation and has slight increase in pore pressure and finally Abu Roach C which is our reservoir where the pore pressure increase suddenly.**(Table 2).**

5. Relation between pore pressure evaluation and hydrocarbon saturation:

Two pore pressure distribution maps were made (using drilling exponent and using Eaton's resistivity) **(Figs.8 and 9)**, they both showed that pore pressure increase towards the centre of the studied area and decrease outward. When the hydrocarbon saturation map **(Fig.6)** is compared with pore pressure distribution maps **(Figs.8 and 9)**, they showed similarity to each other in which both parameters increase towards the centre of the studied area and decreases outward.

Table 2. Average pore pressure values For Abu Roach Formation in the studied area.

Method	Zone	Bed 15-1	Bed 15-3	Bed 15-7	Bed 15-9
Eaton's drilling exponent	Abu Roach A (Seal)	4448.44	4314.37	4283.56	4279.88
	Abu Roach B (Transition)	4713.86	4572.57	4400.28	4417.52
	Abu Roach C (Reservoir)	4762.51	4763.18	4564.27	4585.47
Eaton's Resistivity	Abu Roach A (Seal)	4417.52	4299.41	4568.45	4444.72
	Abu Roach B (Transition)	4519.89	4512.8	4613.36	4522.89
	Abu Roach C (Reservoir)	6009.03	6387.54	5474.66	5513.9

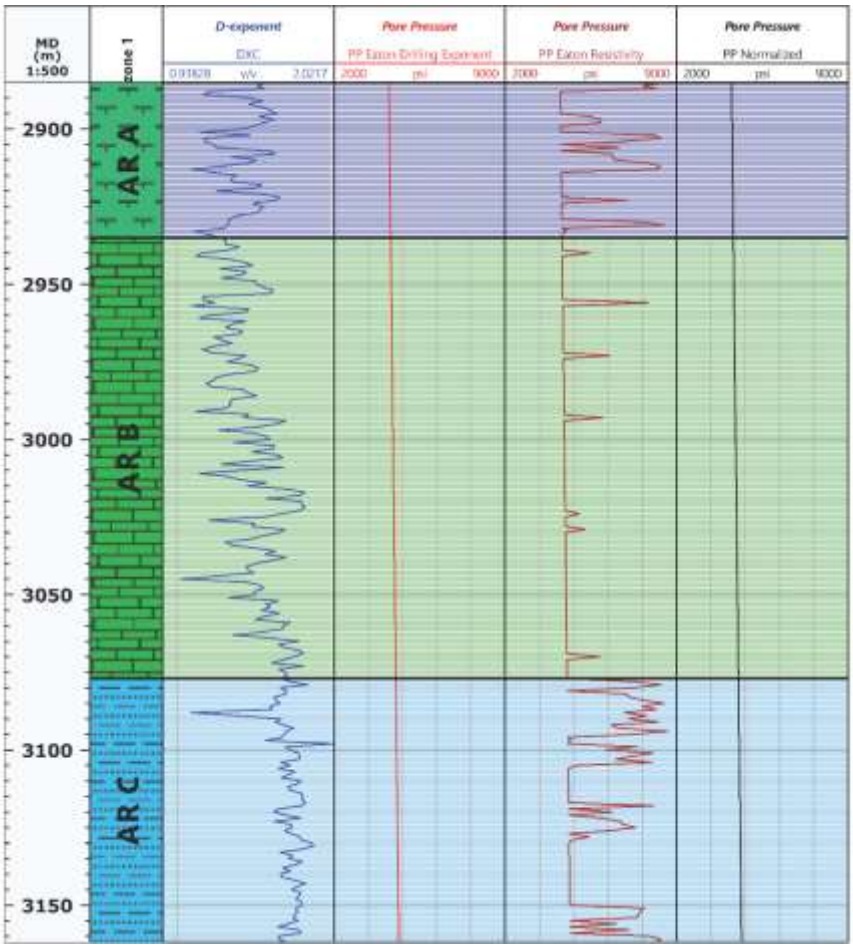

Fig. 7. Pore Pressure Lithostratigraphic Crossplot for Bed 15-1 Well.

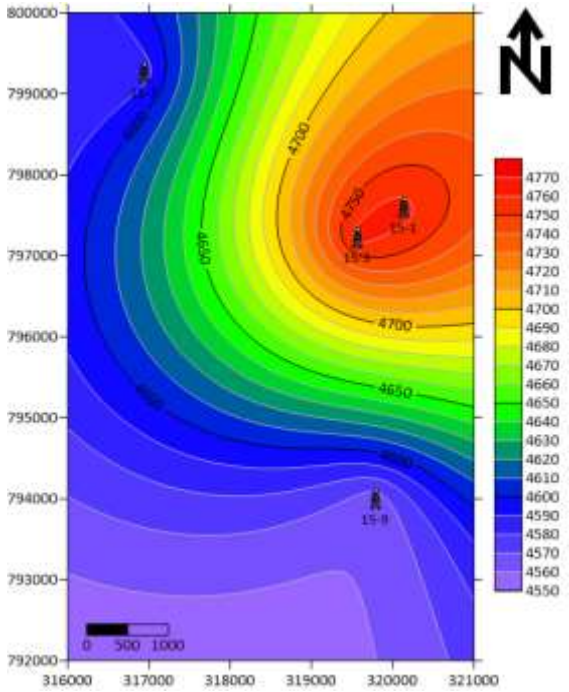

Fig. 8. Pore pressure distribution map of Abu Roach C using Drilling exponent of the studied area.

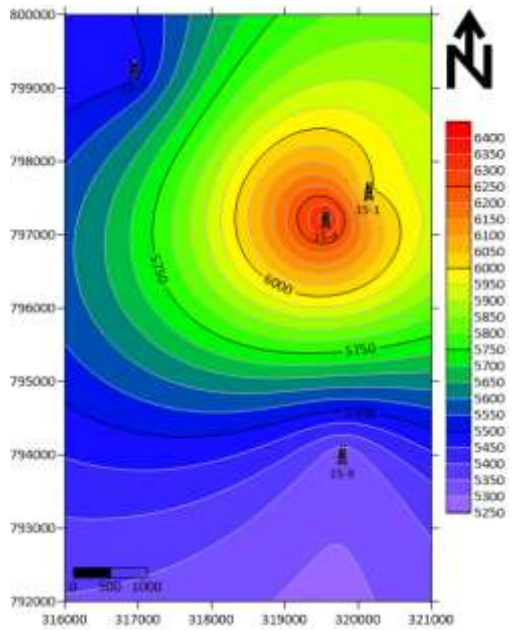

Fig. (9) Pore pressure distribution map of Abu Roach C using Eaton's Resistivity of the studied area

6- Conclusion:

The case study presented in the paper focuses on the Bed-15 oil Field, located in the North-Western region of the Abu Gharadig sedimentary basin within the Egyptian Western Desert. The Bed-15 Field spans across latitudes 29° 45' to 30 ° 05' N

and longitudes 27° 30' to 28° 10' E. and considered a component of the Badr El-Din Concession, which is situated approximately 300 km west of Cairo and around 100 km west of the Bed-1 location.

Well log Formation evaluation was used on Bed 15-1, Bed 15-3, Bed 15-7, Bed 15-8 and Bed 15-9 wells to determine shale volume, total porosity, effective porosity, water saturation and hydrocarbon saturation and then make Litho-saturation Crossplot for the wells and Isoparametric maps for the reservoir which showed that the average reservoir parameter was as follows: the shale volume ranges between 24.4 to 34.2 %, effective porosity ranges from 15 to 23.1% and at last hydrocarbon saturation ranges from 7.7 to 45.8%.

Also pore pressure estimation of Abu Roach Formation using drilling exponent and Eaton's resistivity in the area of study on Bed 15-1, Bed 15-3, Bed 15-7and Bed 15-9 well showed that it can be classified into 3 different zones that showed different pore pressure behaviour. **Abu Roash A** which consist of impermeable shale and has a normal pressure zone which can be considered as the seal of our reservoir, **Abu Roach B** which consists of limestone, shale and sandstone intercalation and has slight increase in pore pressure which can be considered as a transition zone and **Abu Roach C** (our reservoir) which consists of sand with traces of shale and has abnormal pore pressure.

The analysis of pore pressure distribution and hydrocarbon saturation maps showed a direct relation in which as pore pressure increase towards the center of the studied area the hydrocarbon saturation increases.

References

A.Z. NOAH and T. F. Shazly, (2014) Integration of Well Logging Analysis with Petrophysical Laboratory Measurements for Nukhul Formation at Lagia-8 Well, Sinai, Egypt. American Journal of Research Communication, 2 (2), 139-166

Archie, G.E. (1942) The Electrical Resistivity Log as an Aid in Determining Some Reservoir Characteristics. Transactions of the AIME, 146, 54-62.

Awad, G. M., (1984): Habitat of oil in Abu Gharadig and Fayoum basins, Western Desert, Egypt. AAPG. Bull., 68 (5), 564-573.

Barakat, M.G. and Darwish, M., (1987) Stratigraphy of The Lower Cretaceous Sequence in Mersa Matruh Area, North Western Desert, Egypt. M.E.R.C., Ain Shams Univ., Earth Sci. Series. 1, 48-66.

Bingham, M.G. (**1964)** A New Approach to interpreting Rock Drillability, The Petroleum Publishing Co.

Bourgoyne, A.T.J., et al., (1986) Applied Drilling Engineering, SPE Text-book Series, SPE, Richardson, TX.

Dresser Atlas (1979) Log interpretation charts. Dresser Industries Inc., Houston. PP. 107.

Eaton BA (1975) The equation for geopressure prediction from well logs. In: Fall Meeting of the Society of Petroleum Engineers of AIME.

El Gazzar, A., Moustafa, A. & Bentham, P. (2016) Structural evolution of the Abu Gharadig Field area, northern Western Desert, Egypt. Journal of African Earth Sciences, 124**,** 340-354.

El-Gezeery, M.N., Mohesn, S. And Farid, M., (1972) Sedimentary Basins of Egypt and Their Petroleum Prospects 8th Arab Prt.; Cong. Algiers, Paper. N. 83(B-3), 13. Explo. Conf., EGPC, Cairo, Egypt, 31p.

Hantar, G., (2017) North Western Desert. In: The Geology of Egypt. R. Said (Ed. 2017), The Geology of Egypt, Balkema, Rotterdam, PP. 293-319.

Jorden J. R., & Shirley, O. J. (1966) Application of drilling performance data to overpressure detection. J. Petroleum Technology, PP. 1387-1394.

Poupon, A., and Leveaux, J., (1971) Evaluation of water saturation in shaly Formations. The Log Analyst. 12 (4), 1-2.

Rehm and Mcledon (1971) Measurement of Formation Pressure from Drilling Data. SPE 3601, 1971, SPE Reprint Series No. 6a, 1971 Revision.

Said, R. (Ed), (2017) The Geology of Egypt. Routledge, PP. 377.

S**chlu1nberger, (1972b)** Log interpretation, vol. I, principles. Paris, France

S**chlumberger, (1987)** Log interpretation, Principles/ Applications. Schlumberger Educational Service, Houston, Texas 770 I 0, USA. 189P

Schlumberger (1997) Log Interpretation Charts, Schlumberger, Well services. Pans, France.

Schlumberger (2004) Well Services Manual; Log Interpretation Principles, **1**: 1-6

Shalaby, M. R., Hakimi, M. H. & Abdullah, W. H. (2013) Modeling of gas generation from the Alam El-Bueib Formation in the Shoushan Basin, northern western Desert of Egypt. International Journal of Earth Sciences, 102**,** 319-332.

Simandoux, P., (1963) Dielectric measurements in porous media and application to shaly Formation: Revue de L'Institut Français du Pétrole, 18, Supplementary Issue, 193–215.

Sultan, N. & Abdel Halim, M. (**1988**): Tectonic Framework of Northern Western Desert, Egypt and Its Effect on Hydrocarbon Accumulations. Proceedings Of the EGPC 9th Exploration and Production Conference, Cairo. Egyptian General Petroleum Corporation Bulletin, 1-19.

T.F. Shazly, A.Z. Nouh, (2012) Utilizing of Resistivity Log to Discriminate Between Effective and Ineffective Porosity for Raha Formation in Ras Budran Field, Gulf of Suez, Egypt. Australian Journal of Basic and Applied Sciences, 6 (10), 532-540. ISSN 1991-8178

T.F. Shazly, M. Ghorab, I.E. Ghaleb, I. Nabih, (2013) Estimation of the Suitable Water Saturation Model of Bahariya Formation in Sidi Barani Area, Nnorth Western Desert of Egypt by Using Well Logs Analysis. International Journal of Academic Research, Baku, Azerbaijan, 5 (5), 35-49.

العلاقة بين تقييم ضغط المسامي والتشبع الهيدروكربوني لمتكون أبو رواش بحقل ١٥ بدر الدين، الصحراء الغربية، مصر

أحمد مصطفى طلعت[١]، وعصام السيد[٢]، ومحمود غراب[١]، ومحمد عبدالفتاح[١]، وأحمد زكريا نوح[١]

[١] قسم الاستكشاف، معهد بحوث البترول، القاهرة، مصر

[٢] قسم الجيولوجيا، كلية العلوم، جامعة المنيا، مصر

حقل بترول Bed−15 والذي يقع في المنطقة الشمالية الغربية من حوض أبوالغراديج الرسوبي داخل الصحراء الغربية المصرية. يمتد حقل Bed−15 عبر خطوط العرض '45 °29 إلى '05 ° 30 شمالاً وخطي الطول '30 °27 إلى '10 °28 شرقًا، ويعتبر أحد مكونات منطقة امتياز بدر الدين، التي تقع على بعد حوالي ٣٠٠ كم غربًا من القاهرة وعلى بعد حوالي ١٠٠ كيلومتر غرب موقع Bed15−1 موضوع البحث هو متكون أبو رواش، باستخدام مجموعة من البيانات البتروفيزيائية وتحليل تسجيلات الآبار والدراسات الجيولوجية تحت السطحية لفهم الهيدروكربونات المحتملة في تكوين أبو رواش بحقل بدر ١٥ باستخدام ٥ آبار (Bed15−1, Bed15−3, Bed 15−7, Bed15−8 and Bed15−9)، تكوين أبو رواش تم تحديد أنواع مختلفة من المعايير البتروفيزيائية (المسامية وحجم الصخر الزيتي والتشبع المائي والهيدروكربوني). تم اختيار أربعة آبار (Bed15−1, Bed15−3, Bed 15−7 and Bed15−9) لتقييم ضغط المسامي لتكوين أبو رواش باستخدام معاملات الحفر (Dxc) وتسجيلات الأبار. ولوحظ وجود علاقة بين ضغط المسامي والتشبع الهيدروكربوني في المنطقة قيد الدراسة.